Supporting Information

Ester Cross-linking Enhanced Hydrophilic Cellulose Nanofibrils Aerogel

Yulong Li[†], Yushang Liu[†], Yang Liu[†], Wenchuan Lai[†], Feng Huang[†], Anping Ou[†], Rui Qin[†], Xiangyang Liu[†], Xu Wang*[†]*

†State Key Laboratory of Polymer Materials Engineering, College of Polymer Science and Engineering, Sichuan University, No.24 South Section 1, Yihuan Road, Chengdu, Sichuan, 610065, P.R. China.

* Corresponding author.

*Xu Wang, E-mail: wangxu@scu.edu.cn

*Xiangyang Liu, E-mail: lxy@scu.edu.cn

Number of pages: 15
Number of figures: 8
Number of tables: 4

Specific Experimental Steps for Preparing CNFs Raw Materials

100 g of the pre-treated softwood bleaching kraft pulp was formulated with distilled water to a 1% concentration mixture. The mixture was then oxidized by TEMPO/NaBr/NaClO oxidation. The amount of TEMPO was 0.016 g/g of fiber; the amount of NaBr was 10% of fiber and the amount of NaClO was 8 mmol/g of fiber. The oxidation process was carried out for 1 hour at room temperature while maintaining the pH at 10. The oxidized mixture was washed to neutral with distilled water and then set to a certain concentration. Finally, it was homogenized 6 times with a high pressure homogenizer under the pressure of 80 Mpa to obtain a translucent CNFs gel.

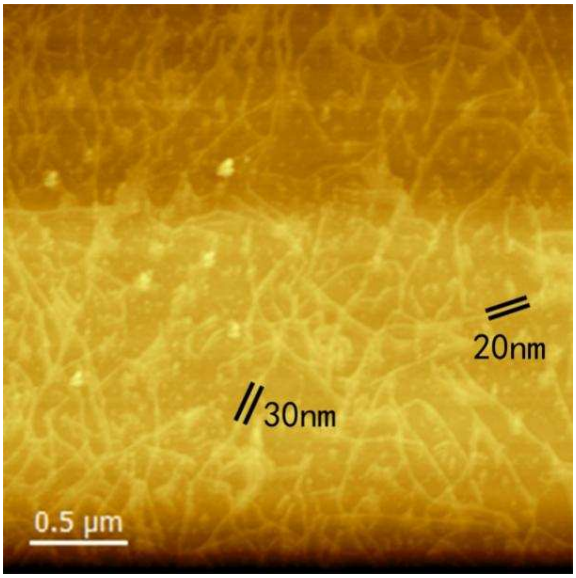

Figure S1. AFM image of CNFs.

Atomic Force Microscopy

Atomic Force Microscopy (AFM) test was carried out by using the SmartSPM instrument (AIST-NT, Inc., Novato CA, USA). For AFM test, the Si wafer was immersed in CNFs suspensions with a concentration of 0.8 mg/ml for seconds and then dried under vacuum at 60 °C for 2 hours. Finally, the prepared silicon wafer loaded with CNFs was tested using the AFM tapping mode.

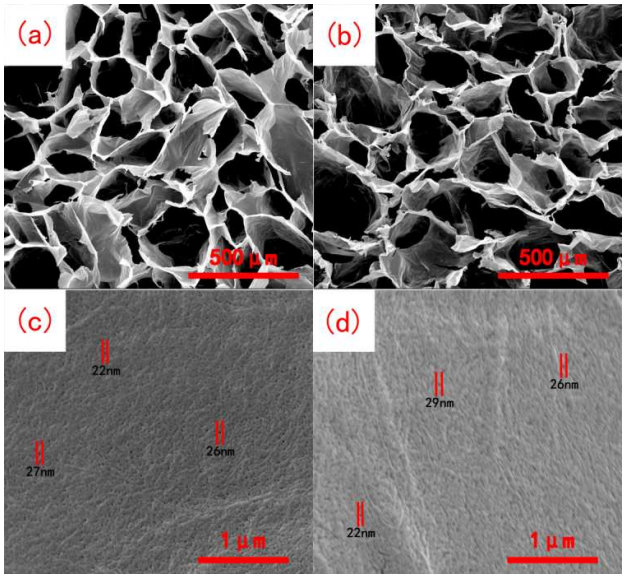

Figure S2. SEM images of CNFs aerogel (a, c) and F-CNFs aerogel (b, d).

Scanning Electron Microscopy

The surface morphology of aerogel was examined using scanning electron microscopy (SEM; FEI Co., Hillsboro, OR, USA).

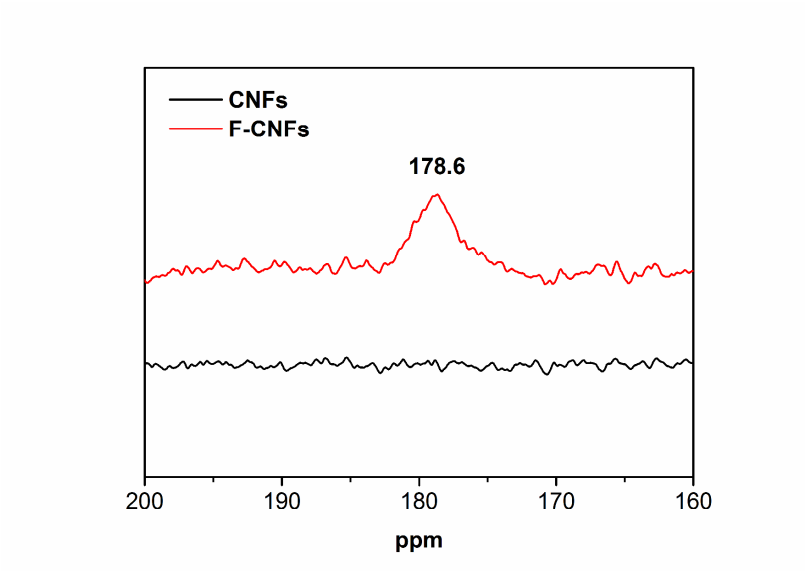

Figure S3. ^{13}C NMR images of CNFs and F-CNFs.

Solid-State Nuclear Magnetic Resonance (^{13}C CP MAS ssNMR)

^{13}C NMR experiments were performed on Agilent 600 DD2 spectrometre at a resonance frequency of 150.81 MHz. 6mm probe CPMAS experiments were performed with a delay time of 3s and a contact time of 1 ms. Scans：6000.

As shown in Figure S6, it's obvious that the spectrum of F-CNFs showed a distinct peak at 178.6 ppm. It has been reported in the literature that the absorption peak at this position represents the presence of a carbonyl in cellulose.[1]

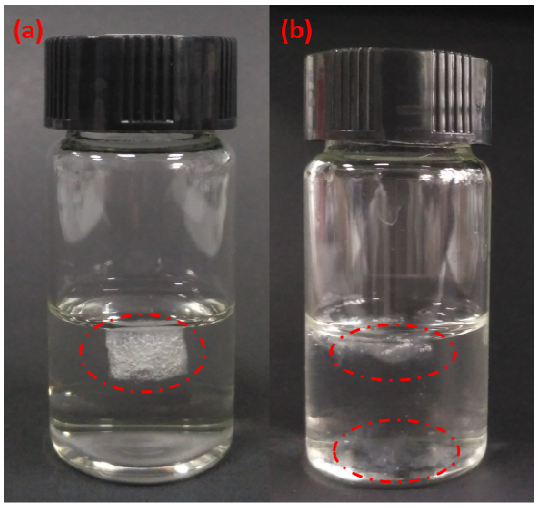

Figure S4. Images of F-CNFs before (a) and after (b) hydrolyzing by alkaline for 12 hours.

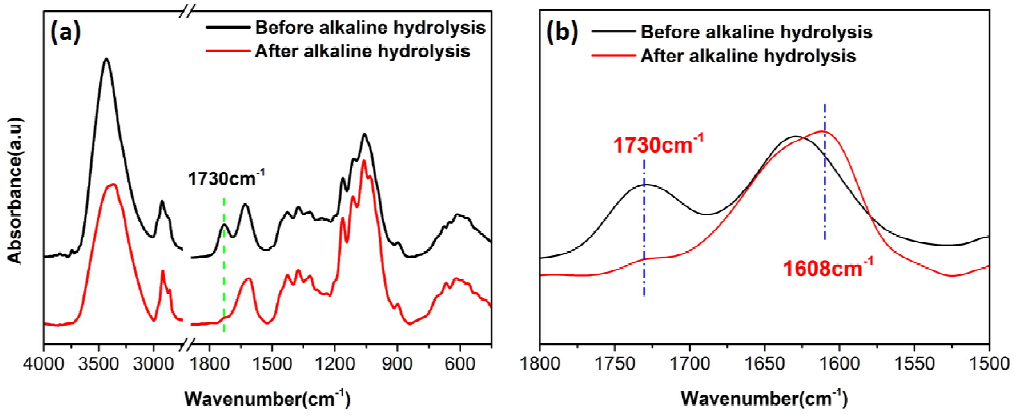

Figure S5. The ATR-FTIR spectra of F-CNFs before and after hydrolyzing by alkaline for 3 days in the range of (a) 4000 cm-1-500 cm-1 and (b)1800 cm-1 -1500 cm-1.

Hydrolysis of F-CNFs Aerogel in Alkaline Solution

In general, ester bonds can be hydrolyzed by strong bases. To demonstrate that our F-CNFs aerogels are crosslinked by ester linkages, we placed the F-CNFs aerogel in a 1 M NaOH solution for hydrolysis. As shown in Figure S3, after standing for 12h in an alkali solution, F-CNFs disintegrated into smaller fragments by mildly swing motion. The fragmentation of F-CNFs in an alkaline solution verified the conjecture of ester-based crosslinking.

In order to structurally investigate the cause of the fragmentation of F-CNFs, we separated the F-CNFs from the alkaline solution after 3 days of hydrolysis and washed to neutrality. After drying hydrolyzed F-CNFs, we measured the ATR-FTIR spectrum of hydrolyzed F-CNFs and compared it with the ATR-FTIR spectrum of unhydrolyzed F-CNFs. As shown in Figure S4, it can be seen that the infrared absorption peak at 1730cm^{-1} of hydrolyzed F-CNFs was greatly reduced compared to that of unhydrolyzed F-CNFs. At the same time, the hydrolyzed F-CNFs showed an obvious increase at the position of 1608 cm^{-1}, which has beem reported as the absorption peak of the carboxylate.[2] This demonstrates that the fragmentation of F-CNFs in an alkaline solution is due to hydrolysis of its ester bond. [3]

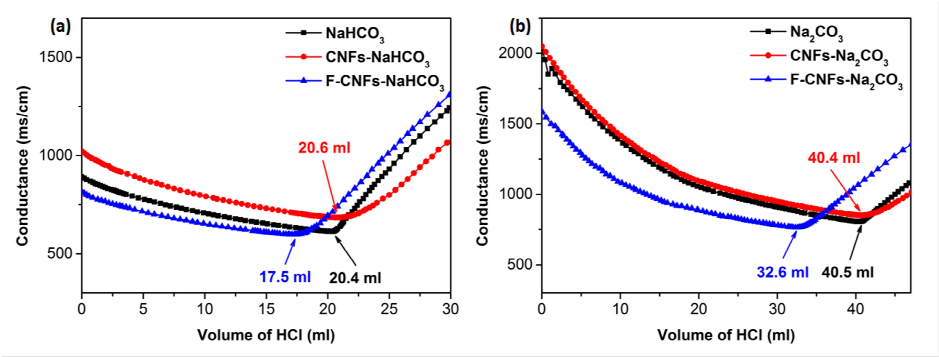

Figure S6. Conductometric titration curves of $NaHCO_3$ (a) and Na_2CO_3 (b) titrated with HCl before and after reacting with CNFs and F-CNFs.

Determination of Surface Carboxyl Groups and Ester Groups

Na_2CO_3 can react with carboxyl groups and ester groups, while $NaHCO_3$ can only react with carboxyl groups due to its weak basicity. Therefore, the two alkaline solutions can be respectively reacted with F-CNFs, and these two alkali solutions after the reaction are titrated with HCl to calculate the content of carboxyl groups and ester groups in the sample.

The F-CNFs were dried under vacuum at 60 ° C for 12 h, and 100 mg of the dried F-CNFs were added to 50 ml 0.01 mol/L $NaHCO_3$ solution. The mixture was magnetically stirred for 2 h and then sonicated for 1 h. The mixture was then sealed and allowed to stand for 3 days to allow it to fully react. After the mixture was centrifuged at 10,000 rpm for 10 minutes, a supernatant of the mixture was obtained. The supernatant was then filtered through a 0.22 micron filter paper to obtain a filtrate and labeled as F-CNFs-$NaHCO_3$. According to the same method, we prepared CNFs-$NaHCO_3$ filtrates. Then the 0.01 mol/L $NaHCO_3$ was replaced by 0.01 mol/l Na_2CO_3 solution, and the F-CNFs-$NaHCO_3$ and CNFs-Na_2CO_3 filtrates were obtained

by the same method.

20 ml $NaHCO_3$ solution was titrated with a 0.01 mol/L HCl solution to obtain a reference curve, and the volume of HCl consumed was recorded as V1. Then 20 ml F-CNFs-$NaHCO_3$ filtrates were titrated with the same HCl solution to obtain the corresponding titration curve, and the volume of HCl consumed by F-CNFs-$NaHCO_3$ was recorded as V2. The content of the carboxyl group in the F-CNFs can be calculated by the fallowing formula:

C_{COOH} (mmol/g) = 0.25× (V1 - V2).

The content of ester and carboxyl groups in F-CNFs can be determined by titrating the F-CNFs-Na_2CO_3 filtrates by the same titration method. Then, the content of the ester group in the F-CNFs can be calculated. The CNFs-$NaHCO_3$ filtrates and CNFs-Na_2CO_3 filtrates were titrated in the same way.

As can be seen from Figure S5, the volume of HCl consumed by F-CNFs-$NaHCO_3$ is 17.5 ml, which is obviously smaller than that of $NaHCO_3$ (20.4 ml), while the volume of HCl consumed by CNFs-$NaHCO_3$ was very close to the volume of HCl consumed by $NaHCO_3$. This indicates that the content of unionized carboxyl groups in F-CNFs is high, and thus the unionized carboxyl groups in F-CNFs consumed much $NaHCO_3$, while the content of unionized carboxyl groups in CNFs is small.

Correspondingly, the volume of HCl consumed by the F-CNFs-Na_2CO_3 is smaller than the volume of HCl consumed by Na_2CO_3, while the volume of HCl consumed by CNFs-Na_2CO_3 is not much different from the volume of HCl consumed by Na_2CO_3.

This indicates that there are fewer carboxyl groups and ester groups in the CNFs, while the content of unionized carboxyl and ester groups in F-CNFs is relatively high.

By calculation, we obtained the content of carboxyl groups in F-CNFs as c (COOH) = 0.25 × (20.4-17.5) = 0.725 mmol / g, and the total content of the ester group and the carboxyl group was c (COOH + COOC) = 0.25 × (40.5-32.6) = 1.975 mmol / g. Furthermore, it was known that the ester group content in F-CNFs is c (COOC) =c (COOH+COOC) – c (COOH) = 1.250 mmol / g. From the titration results, we can see that the content of carboxyl and ester groups in the F-CNFs treated by fluorination is significantly increased compared to CNFs. This further demonstrates the increase in carboxyl groups and the formation of ester-based cross-linking points in F-CNFs.

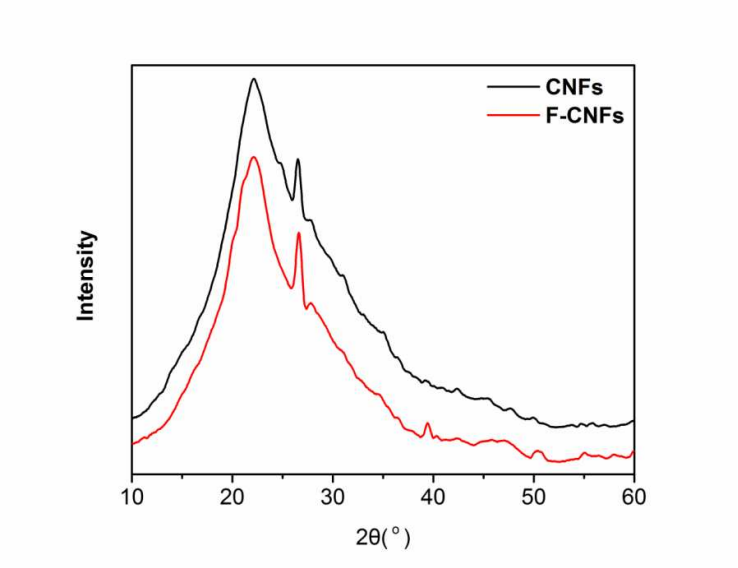

Figure S7. XRD spectra of CNFs and F-CNFs.

X-Ray Diffraction

XRD patterns were acquired at room temperature from Ultima IV powder diffractometer (Rigaku Corporation) using Cu Kα radiation (k = 0.154 nm, U =40 kV, I = 40 mA) over the angular range 5–70° with a step size of 0.02°.

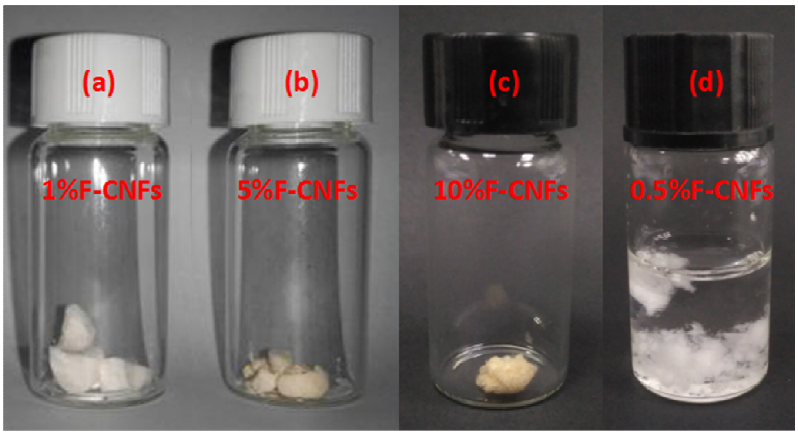

Figure S8. (a, b and c) Images of F-CNFs aerogels treated with different concentration of F_2 and (d) image of F-CNFs disintegrating in water. The 1%F-CNFs, 5%F-CNFs, 10%F-CNFs and 0.5%F-CNFs represent the F-CNFs treated by mixture gas (F_2 and N_2) with the volume fraction of F_2 of 1%, 5%, 10% and 0.5% respectively.

Optimization of the Fluorination Process

Since F_2 is very active and easily reacts with the polymer, we chose to carry out the fluorination treatment at room temperature. We have mainly explored the effect of fluorine concentration on the F-CNFs materials. To this end, we have selected four different concentrations of F_2 to treat our CNFs aerogels, and the volume fraction of fluorine gas we chosen are 0.5%, 1%, 5% and 10%. The F-CNFs treated by mixture gas (F_2 and N_2) with the volume fraction of F_2 of 1%, 5%, 10% and 0.5% are remarked as 1%F-CNFs, 5%F-CNFs, 10%F-CNFs and 0.5%F-CNFs, respectively. The color of F-CNFs gradually deepened with the increase of F_2 concentration (as shown in the Figure S7a, 7b and 7c). Furthermore, 5%F-CNFs and 10%F-CNFs were very brittle，which indicate that the structure of F-CNFs may be severely damaged. For 0.5%F-CNFs, it was easily disintegrated in water (Figure S7d). However, 1% F-CNFs owned best mechanical properties and its water resistance was greatly

improved. So the final volume fraction of fluorine gas we chosen was 1%.

Specific Analysis Process for the Possible Reason of Bigger Nano-pore in F-CNFs

The results of BET indicate that the size of nano-pore in F-CNFs increased from 3.1 nm to 5.6 nm. For this change, we propose two possible reasons: the bigger nano-pore was attributed to 1) severe corrosion of F-CNFs or 2) the short crosslinks of ester bonds formed in F-CNFs.

However, if the increase of nanopores is caused by corrosion, the compression performance of F-CNFs is difficult to be improved. In addition, the results of FTIR and XPS indicate that the skeleton of cellulose is not destroyed. We have measured the weight of the aerogel before and after the treatment in the dry state, and found that the mass of F-CNFs decreased by 1.6% after fluorination. A small drop in mass indicates that F-CNFs have not been highly corroded. These evidences indicated that F-CNFs have not experienced serious corrosion.

Since fluorine gas is a gaseous small molecule, it is likely for F_2 to enter the space between the cellulose nanofibers, which may promote the oxidation of the hydroxyl groups to form ester-linking points between cellulose nanofibers. Then the hydrogen bonding interaction between the cellulose nanofibers were replaced by ester linkage crosslinks. Since the length of the covalent cross-linking point of the ester group is shorter than the hydrogen bond interaction, the distance between the nanofibers may become smaller. The aggregation between CNFs by formation of

ester-linking points facilitates the enhancement of mechanical properties of F-CNFs aerogel. Simultaneously, the above structure evolution results in that the Nano-sized pores within the CNF aerogels became bigger.

Table S1. Specific surface area and hole size of CNFs and F-CNFs.

Samples	Surface Area（m^2/g）	Pore Diameter(nm)
CNFs	139	3.1
F-CNFs	97	5.6

Table S2. The external element analysis of CNFs and F-CNFs measured by XPS.

Samples	Element content (at. %)			Element Ratio	C*-C (284.6)	C*-OH (286.3)	O-C*-O C*=O (288.1)
	C	O	F	O/C (±0.01)			
CNFs	62.01	37.99	0	0.61	41.08%	47.16%	11.76%
F-CNFs	65.26	34.74	0	0.53	41.36%	40.70%	17.94%

Table S3. TGA and DTG analysis of CNFs and F-CNFs.

Samples	$T_{10\%}$ [a] (℃)	T_{max}(℃)	WLR_{max} [b] (%℃$^{-1}$)	CY(%）
CNFs	230	311	-6.6	20.4
F-CNFs	239	342	-6.8	17.2

[a] $T_{10\%}$ is the temperature at 10% weight loss

[b] WLR_{max} is the maximum weight loss rate

Table S4. The water absorption performance of F-CNFs aerogels with different densities.

Samples	Concentration （wt.%）	Density （mg/cm^3）	Water absorption (g/g)	Shape recovery time（s）
F-LCNFs	0.5%	10.39	123.65	4
F-HCNFs	1%	17.31	56.21	2

References:

1. Spinella, S.; Maiorana, A.; Qian, Q.; Dawson, N. J.; Hepworth, V.; McCallum, S. A.; Ganesh, M.; Singer, K. D.; Gross, R. A., Concurrent Cellulose Hydrolysis and Esterification to Prepare a Surface-Modified Cellulose Nanocrystal Decorated with Carboxylic Acid Moieties. *ACS Sustainable Chemistry & Engineering* **2016,** *4* (3), 1538-1550.
2. Da, S. P. D.; Montanari, S.; Vignon, M. R., TEMPO-mediated oxidation of cellulose III. *Biomacromolecules* **2003,** *4* (5), 1417-1425.
3. Liu, L.; Sun, J.; Li, M.; Wang, S.; Pei, H.; Zhang, J., Enhanced enzymatic hydrolysis and structural features of corn stover by FeCl3 pretreatment. *Bioresour Technol* **2009,** *100* (23), 5853-8.